Asian Journal of Chemistry; Vol. 37, No. 7 (2025), 1629-1635

ASIAN JOURNAL OF CHEMISTRY

https://doi.org/10.14233/ajchem.2025.33839

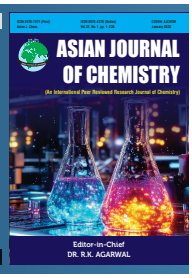

Structural, Magnetic, Resistivity and Magnetoresistance Studies on $Sr_{2-x}Ba_xFeMoO_6$ (x = 0, 1 and 2) Double Perovskites

A. Manjula Devi[1,2,*], Y. Markandeya[3], G. Rajender[4] and R. Balaji Rao[2]

[1]Department of Physics, A.V. College of Arts, Science and Commerce, Gaganmahal, Hyderabad-500029, India
[2]Department of Physics, GITAM School of Technology, Hyderabad-502329, India
[3]Department of Physics, Nizam College, Osmania University, Hyderabad-500001, India
[4]Department of Physics, Osmania University, Hyderabad-500007, India

*Corresponding author: E-mail: manjula.aruva@gmail.com

Received: 8 April 2025; *Accepted*: 31 May 2025; *Published online*: 30 June 2025; AJC-22036

Double perovskite $Sr_{2-x}Ba_xFeMoO_6$ (x = 0, 1 and 2) (SBFMO) materials were synthesized by sol-gel technique in the presence of H_2/Ar atmosphere at 1050 ºC. From X-ray analysis, it was observed that these double perovskite SBFMO materials crystallized in tetragonal structure for the composition x = 0 and, in cubic structure for composition x = 1 and 2. The coercivity (H_c), saturation magnetization (M_s) and remanent magnetization (M_r) of SBFMO samples were evaluated from magnetic measurements. The variation in electrical resistivity (ρ) within the temperature range of 5-300 K was done, by which semiconductor to metallic transformation has been detected in SBFMO sample. The Magnetoresistance (MR, %) was assessed with changes in temperature and magnetic field, revealing that the MR (%) values of SBFMO samples differ from the composition x = 1.

Keywords: Double perovskite, Sol-gel, Crystal structure, Magnetization, Magnetoresistance.

INTRODUCTION

Double perovskite materials have attracted considerable interest in recent years owing to their distinctive structural adaptability and adjustable physical characteristics. Numerous researches in the scientific literature have established that these materials exhibit a broad spectrum of intriguing applications across diverse domains, including spintronics, photovoltaics, catalysis, energy storage and optoelectronics [1-6]. $C_2DD'O_6$ represents the composition of double perovskites, where alkaline earth elements are indicated by C, transition-metal elements with +3 or +2 oxidation states are represented by D, transition-metal elements with +5 or +6 oxidation states are denoted by D′ and oxygen is symbolized by O.. The magnetic, transport as well as magneto resistance characteristics of many types of double perovskite depend on the selection of D and D′ atoms in the magnetic interaction of D-O-D′ [4]. The $C_2DD'O_6$ double perovskite form a tetragonal and cubic structure that has a space group $I4/mmm$ and space group $Fm\bar{3}m$, respectively [1,7].

In the structure of $C_2DD'O_6$ material, regular arrangement of corner-sharing DO_6 and $D'O_6$ octahedra are alternatively present continuously in the three-directional space of the crystal, apart from this, the spaces between the DO_6 and $D'O_6$ octahedra are occupied by cation C [1,6]. The properties of materials like characterization, magnetoresistance and magnetic attributes of C_2FeMoO_6 (where C = Sr, Ba and Ca) have been comprehended, and are synthesized using the solid-state method [2-8]. From previous reports on such materials, it is inferred that sol-gel technique was not used in preparation. The present work has been designed to study the structure, magnetic, magnetoresistance of $Sr_{2-x}Ba_xFeMoO_6$ (x = 0, 1 and 2) by sol-gel preparation technique.

EXPERIMENTAL

The $Sr(NO_3)_2$, $Ba(NO_3)_2$, H_2MoO_4 and $Fe(NO_3)_3{\cdot}9H_2O$ were used for preparing of $Sr_{2-x}Ba_xFeMoO_6$ (x = 0, 1 and 2). The entire procedure to prepare the SBFMO materials are followed from the literature [5,9-11]. In this method, $Sr_{2-x}Ba_xFeMoO_6$

(x = 0, 1 and 2) samples were inserted into a tubular furnace at around 1050 ºC in the presence of gas flow (H_2-Ar) for 12 h to convert the ionic state from Mo^{6+} to Mo^{5+} in SBFMO. The crystal structures of $Sr_{2-x}Ba_xFeMoO_6$ (x = 0, 1 and 2) were confirmed by X-ray diffractometer. Room temperature magnetization measurements of the SBFMO samples were done in the magnetic field which ranges from -15 kOe to 15 kOe with the help of vibration sample magnetometer. Electrical resistivity measurements of SBFMO sample were prepared in the temperature range from 5 to 300 K at different constant magnetic fields 0 kOe, 20 kOe, 40 kOe, 50 kOe and 80 kOe with the help of superconducting magnetic system employing the standard four-probe technique. Variations in the electrical resistivity of SBFMO were also measured at different temperatures *viz*. 5 K, 150 K and 300 K in the magnetic field range from 0 kOe to 80 kOe. The relative percentage of magnetoresistance of SBFMO samples were evaluated in both cases, varying temperature as well as magnetic field and by using the data of electrical resistivity in presence and absence of a magnetic field.

RESULTS AND DISCUSSION

X-ray diffraction: The X-ray diffraction (XRD) patterns of $Sr_{2-x}Ba_xFeMoO_6$ (x = 0, 1 and 2) materials recorded at room temperature (Fig. 1). The X-ray diffractograms of SBFMO were analyzed and compared with previous literature [4-6]. It is confirmed from X-ray analysis that the composition x = 0 and x = 1, 2 crystallize in tetragonal and cubic structure that has a space group $I4/mmm$ and space group $Fm\bar{3}m$, respectively [4-6]. Lattice parameters of $Sr_{2-x}Ba_xFeMoO_6$ samples were evaluated in the method of Cohen's least square, by taking the individual (*hkl*) values and Bragg angle values of the XRD peaks estimated from CELEN computer program [10]. The formulae $V = a^2c$ and $V = a^3$ were used to calculate the volume of the unit cell for tetragonal and cubic structure of $Sr_{2-x}Ba_xFeMoO_6$, respectively. The lattice parameters along with unit cell volumes of these samples are specified in Table-1. It is known from analysis of XRD that the structure of material convert from tetragonal to cubic when Ba atom is inserted in place of Sr atom at C-site in the C_2FeMoO_6 double perovskite [2,6,9, 12,13]. Lattice parameters and unit cell volume of SBFMO increases when composition changes from x = 0 to 2 owing to the size of Ba^{2+}which is bigger than that of Sr^{2+} [4].

Magnetization: Fig. 2 shows the change of magnetization when magnetic field is varied from -15 to 15 kOe at 300 K for $Sr_{2-x}Ba_xFeMoO_6$ (x = 0, 1 and 2) (SBFMO) samples. The values of coercivity (H_c), remanent magnetization (M_r) and saturation magnetization (M_s) of SBFMO samples were evaluated and are specified in Table-1. From Fig. 2, it is clearly observed that the maximum saturation magnetization (M_s) is observed at composition x = 1 and such that it decreases when composition deviates from x = 1 to 0 and from 1 to 2. This might be attribu-

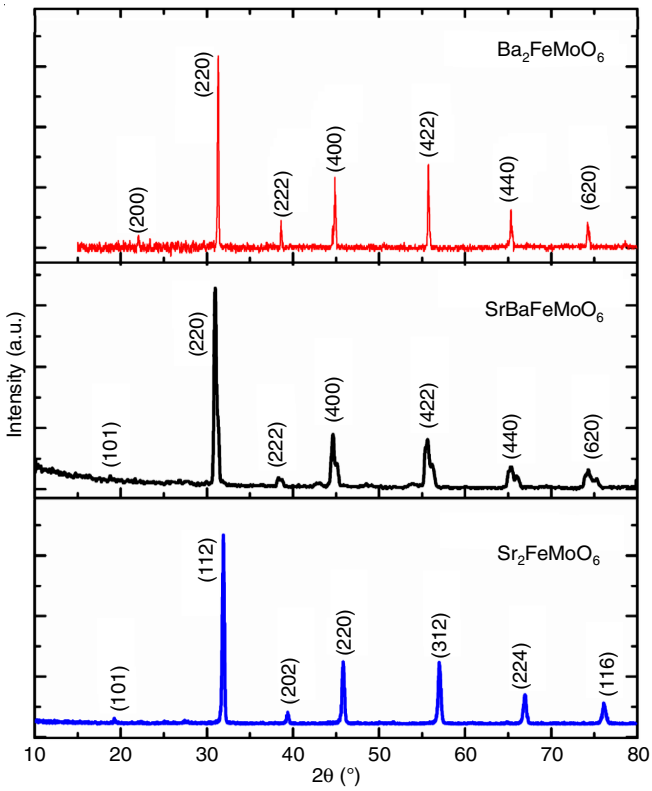

Fig. 1. X-ray diffraction patterns of $Sr_{2-x}Ba_xFeMoO_6$ (x = 0, 1 and 2) samples recorded at room temperature.

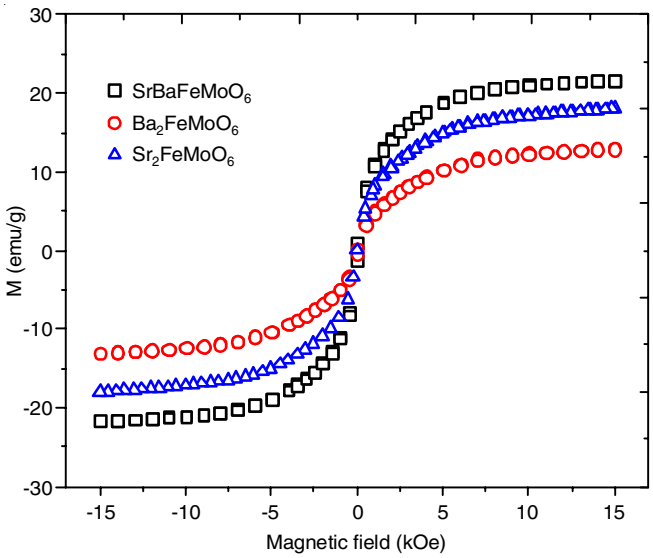

Fig. 2. Magnetic field dependence magnetization (M–H) curves of $Sr_{2-x}Ba_xFeMoO_6$ samples obtained at temperature 300 K

TABLE-1
THE VALUES OF LATTICE PARAMETER (a), UNIT CELL VOLUME (V), SATURATION MAGNETIZATION (M_S), REMANENT MAGNETIZATION (M_r), COERCIVITY (H_C) AND OF $Sr_{2-x}Ba_xFeMoO_6$ (x = 0, 1 AND 2) MATERIALS

Samples	a (Å)	c (Å)	V (Å^3)	M_S (emu/g)	M_r (emu/g)	H_C (kOe)
Sr_2FeMoO_6	5.569	7.898	244.98	18.07	0.32	0.039
$SrBaFeMoO_6$	8.066	–	524.91	21.66	1.29	0.055
Ba_2FeMoO_6	8.073	–	526.14	12.55	0.34	0.038

ted, theoretically that extreme degree of Mo/Fe ordering occurs at composition $x = 1$ in $Sr_{2-x}Ba_xFeMoO_6$ samples. The degree of Mo/Fe ordering generally influences the result of magnetization in the double perovskite materials. In this case, the degree of Mo/Fe ordering decreases the saturation magnetization (M_s) as the composition deviates from $x = 1$. The change in saturation magnetization (M_s) with composition may be further more owed to miss-site imperfection or anti-site defects between Fe and Mo atom, oxygen deficiency and valence disproportion in the $Sr_{2-x}Ba_xFeMoO_6$ samples [2,14,15]. It is also observed from Table-1 that M_r and H_c decrease with composition x and deviate from 1 in $Sr_{2-x}Ba_xFeMoO_6$ due to rise in anti-site defects or else decrease in degree of ordering [2,10,11].

Temperature dependence on electrical resistivity: The resistivity (ρ) as a function of temperature varied from 5-300 K at fixed magnetic fields 0, 10, 20 and 40 kOe is presented in Fig. 3a for composition $x = 0$ (Sr_2FeMoO_6). It is observed that the resistivity at composition $x = 0$ (Sr_2FeMoO_6) vary between 0.5931×10^{-4} to 0.6934×10^{-4} Ω-cm at 0 Oe, 0.5883×10^{-4} to 0.6103×10^{-4} Ω-cm at 10 kOe, 0.5894×10^{-4} to 0.5881×10^{-4} Ω-cm at 20 kOe and 0.5693×10^{-4} to 0.5831×10^{-4} Ω-cm at 40 kOe. The value of resistivity (ρ) in the present analysis is lesser than that earlier reported for Sr_2FeMoO_6 [1]. The method of preparation technique and sintering conditions influences on the resistance of the sample [2,3]. The composition $x = 0$ (Sr_2FeMoO_6) shows two variations in the temperature range from 5-300 K. One is the semiconductor state in lower temperatures and other one is metallic state at higher temperatures. The semi-conductor to metal transition temperature (T_{SM}) values of composition $x = 0$ (Sr_2FeMoO_6) at fixed magnetic fields 0, 10, 20 and 40 kOe were derived from Fig. 3a and are shown in Table-2. The T_{SM} for composition $x = 0$ (Sr_2FeMoO_6) sample reduces by rise in the magnetic field. It might be owed to the diminishing scattering effect thereby increasing in magnetic moment ordering in the sample [11].

The resistivity (ρ) plots of sample at composition $x = 1$ ($SrBaFeMoO_6$) *versus* the temperature from 5-300 K are illustrated in Fig. 3b at fixed magnetic fields of 0, 20, 50 and 80 kOe. The resistivity of composition $x = 1$ ($SrBaFeMoO_6$) by varying temperature 5 to 300 K is in the range 0.265×10^{-4} to 0.391×10^{-4} Ω-cm at constant magnetic field 0 kOe, 0.246×10^{-4} to 0.390×10^{-4} Ω-cm at fixed magnetic field 20 kOe, 0.235×10^{-4} to 0.388×10^{-4} Ω-cm at fixed magnetic field 50 kOe and 0.232×10^{-4} to 0.384×10^{-4} Ω-cm at fixed magnetic field 80 kOe.

The resistivity of $SrBaFeMoO_6$ sample in the non-magnetic field is larger than previously reported [4]. The high value of resistivity of $SrBaFeMoO_6$ can be ascribed to dissimilar synthesis technique and the sintered environment. The $SrBaFeMoO_6$ exhibits a transformation from semiconductor to metallic behaviour by varying temperature (5 to 300 K) in the magnetic field and as well as non-magnetic fields. The semiconductor-metal transition temperature values (T_{SM}) of $SrBaFeMoO_6$ at the fixed magnetic fields 0, 20, 50 and 80 kOe were determined from Fig. 3b and are specified in Table-2. From the results, the values of semiconductor to metallic transition temperature (T_{SM}) fall to minor regime due to rise in the magnetic domain ordering by increasing of the magnetic field intensity [5,10].

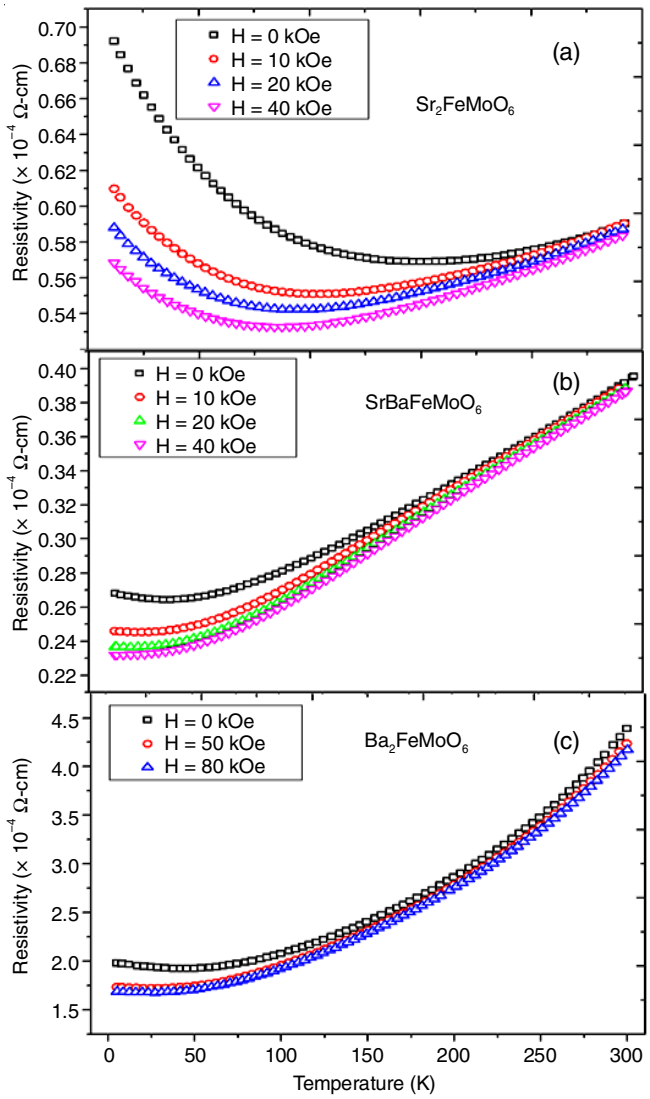

Fig. 3. Electrical resistivity as a function of temperature of $Sr_{2-x}Ba_xFeMoO_6$ ($x = 0$, 1 and 2) samples with different constant magnetic fields

In the temperature variation from 5 to 300 K, resistivity (ρ) of Ba_2FeMoO_6 sample (composition $x = 2$) at the constant magnetic fields of 0, 50 and 80 kOe is illustrated in Fig. 3c. It is found that the resistivity of $BaFeMoO_6$ varies between 2.0 $\times 10^{-4}$ to 4.5×10^{-4} Ω-cm at 0 kOe, 1.8×10^{-4} to 4.3×10^{-4} Ω-

TABLE-2
VALUES OF SEMICONDUCTOR-METALLIC TRANSITION TEMPERATURE (T_{SM}) OF $Sr_{2-x}Ba_xFeMoO_6$ SAMPLES AT DIFFERENT CONSTANT MAGNETIC FIELDS

Samples	Semiconductor-Metallic transition temperature (T_{SM}) in Kelvin at different constant magnetic fields			
Sr_2FeMoO_6	179 K @ 0 kOe	126 K @ 10 kOe	112 K @20 kOe	101 K @ 40 kOe
$SrBaFeMoO_6$	35 K @0 kOe	20 K @ 20 kOe	13 K @50 kOe	–
Ba_2FeMoO_6	46 K@ 0 kOe	27 K @ 50 kOe	26 K @ 80 kOe	–

cm at 50 kOe and 1.7×10^{-4} to 4.2×10^{-4} Ω-cm at 80 kOe by increasing the temperature from 5 to 300 K. In present study, resistivity of Ba_2FeMoO_6 in the non-magnetic fields is lower than the previous reported [6-8]. The lower resistivity of Ba_2FeMoO_6 is due to adopted dissimilar procedure in the preparation technique and sintering temperature. The synthesis environment and grain boundaries of double perovskite have influenced generally on the property of resistivity [4,6,9,10,16,17]. It was found from Fig. 3c that Ba_2FeMoO_6 sample exhibited semiconductor to metallic change in the temperature 5-300 K thereby indicating a semiconductor-metallic transition. The semiconductor-metal transition temperature values (T_{SM}) of the sample were obtained from Fig. 3, which are specified in Table-2. It is seen from Table-2 that the T_{SM} value drops off with raise of magnetic field for Ba_2FeMoO_6 sample. This could be attributed to increase in magnetic domain ordering along with the magnetic field thereby resistivity of Ba_2FeMoO_6 reduced [5,11].

Magnetic field dependence on electrical resistivity: The resistivity (ρ) of $Sr_{2-x}Ba_xFeMoO_6$ ($x = 0$, 1 and 2) samples with variation of magnetic fields from -40 to 40 kOe for composition $x = 0$, -80 to 80 kOe for composition $x = 1$, 2 at fixed temperatures of 5, 150 and 300 K is illustrated in Fig. 4a-c, respectively. The resistivity values of $Sr_{2-x}Ba_xFeMoO_6$ ($x = 0$, 1 and 2) samples are shown in Table-3. From the resistivity values, the resistivity of $Sr_{2-x}Ba_xFeMoO_6$ ($x = 0$, 1 and 2) samples reduces with raise in the magnetic field. The reduction of resistivity with magnetic field could be correlated to the enhancement in the magnetic domain ordering which diminishes electron-magnon collisions [5].

TABLE-3
RANGE OF ELECTRICAL RESISTIVITY WITH VARIATION OF MAGNETIC FIELD AT TEMPERATURES 5, 150 AND 300 K FOR $Sr_{2-x}Ba_xFeMoO_6$ ($x = 0$, 1 AND 2) SAMPLES

Compounds	Range of electrical resistivity (Ω-cm)		
	300 K	150 K	5 K
Sr_2FeMoO_6	$5.84\text{-}5.92 \times 10^{-3}$	$5.38\text{-}5.73 \times 10^{-3}$	$5.69\text{-}6.95 \times 10^{-3}$
$SrBaFeMoO_6$	$3.87\text{-}3.93 \times 10^{-3}$	$2.90\text{-}3.05 \times 10^{-3}$	$3.86\text{-}4.37 \times 10^{-3}$
Ba_2FeMoO_6	$0.42\text{-}0.44 \times 10^{-2}$	$2.29\text{-}2.41 \times 10^{-3}$	$0.17\text{-}0.19 \times 10^{-2}$

Temperature dependence magnetoresistance (MR): The variation of resistance with the influence of magnetic field is well known as magnetoresistance. The percentage of magnetoresistance is defined as:

$$\text{Magnetoresistance } (\%) = \frac{\rho(H,T) - \rho(0,T)}{\rho(0,T)} \times 100$$

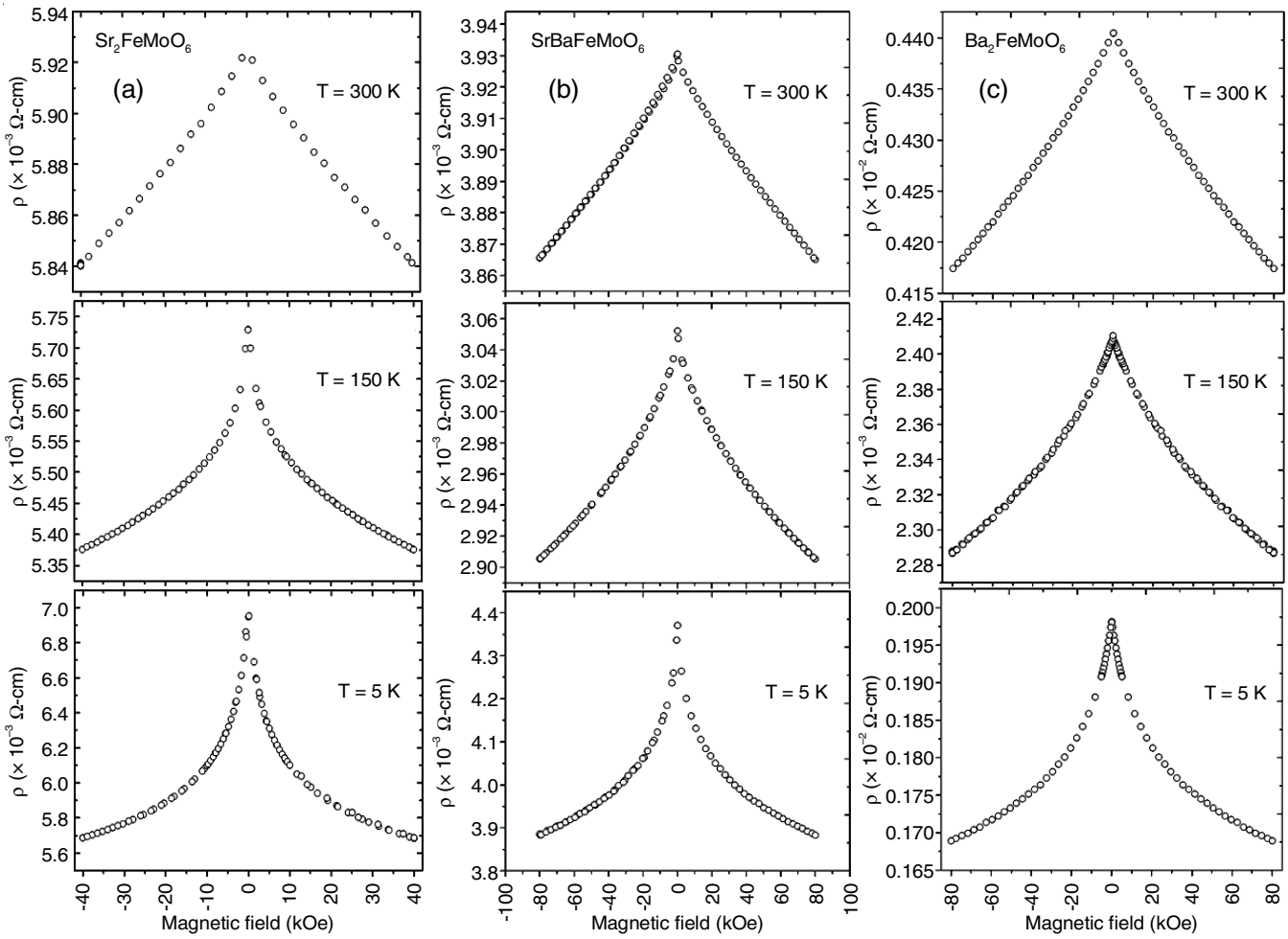

Fig. 4. Electrical resistivity *versus* magnetic field at constant temperatures 5, 150 and 300 K for the composition (a) $x = 0$, (b) $x = 1$ and (c) $x = 2$ of $Sr_{2-x}Ba_xFeMoO_6$

where H is the applied magnetic field, ρ(0,T) is the resistivity's at non-magnetic field and ρ(H,T) is the resistivity at magnetic field H at temperature T. The MR (%) of $Sr_{2-x}Ba_xFeMoO_6$ (x = 0, 1 and 2) with varying temperature from 5-300 K at fixed magnetic fields are shown in Fig. 5a-c. It is observed from Fig. 5a-c that the variation of magnitude of MR (%) of $Sr_{2-x}Ba_xFeMoO_6$ sample increases with a decrease in temperature due to effect of domination of the grain boundaries or effect of magnetic domain boundaries thereby the MR (%) of SBFMO rises with reduction in temperature or in the other way, that decrease of effects of spin-scattering on the region around grain boundaries [1,5,9,18]. It was found from the Fig. 5c that the MR (%) at magnetic field 50 and 80 kOe in the 5-200 K temperature region increases while there is no systematic variation in the 200-300 K temperature region in the Ba_2FeMoO_6 sample.

Magnetic-field dependence magnetoresistance (MR): The MR (%) of $Sr_{2-x}Ba_xFeMO_6$ (x = 0, 1 and 2) samples in the various magnetic field range particular temperatures 5, 150 and 300 K are illustrated in Fig. 6a-c. The MR (%) values are shown in Table-4. It was observed from figure that the MR (%) increases at 5, 150 and 300 K along with increase of magnetic field. This may be due to the lowering of spin-scattering at region of grain boundaries and also, polarization in charge carrier increases with the application of magnetic field [6,8,9,19-21]. This process is most efficient at lower magnetic fields and temperatures lower than Curie temperature, in which case the polarization of charge carriers is comparatively high. Another explanation for the above is an intrinsic one that result from the quenching of spin-scattering of the carriers by localized spins. This process dominates the high magnetic field MR [6,19]. It can be seen from Fig. 6b that the MR (%) of the sample increases rapidly with change in magnetic field from 0 to 20 kOe. And further more the MR (%) slowly increases with variation in the magnetic field from 20 to 80 kOe. In double perovskites, magnetoresistance arise from the penetrating of spin-polarized carriers across the insulating barriers. These barriers can be grain boundaries, Mo-Fe imperfection disorders and also domain walls [4,5,22,23]. Spin polarization of charge carriers play important

TABLE-4
VALUES OF MR (%) OF $Sr_{2-x}Ba_xFeMO_6$ (x = 0, 1 AND 2) SAMPLES AT CONSTANT TEMPERATURES 5,150 AND 300K AND MAGNETIC FIELD 40 kOe

Compounds	MR (%)		
	5 K and 20 kOe	150 K and 40 kOe	300 K and 40 kOe
Sr_2FeMoO_6	-15.54	-6.18	-1.38
$SrBaFeMoO_6$	-17.35	-10.23	-4.12
Ba_2FeMoO_6	-8.48	-3.33	-2.88

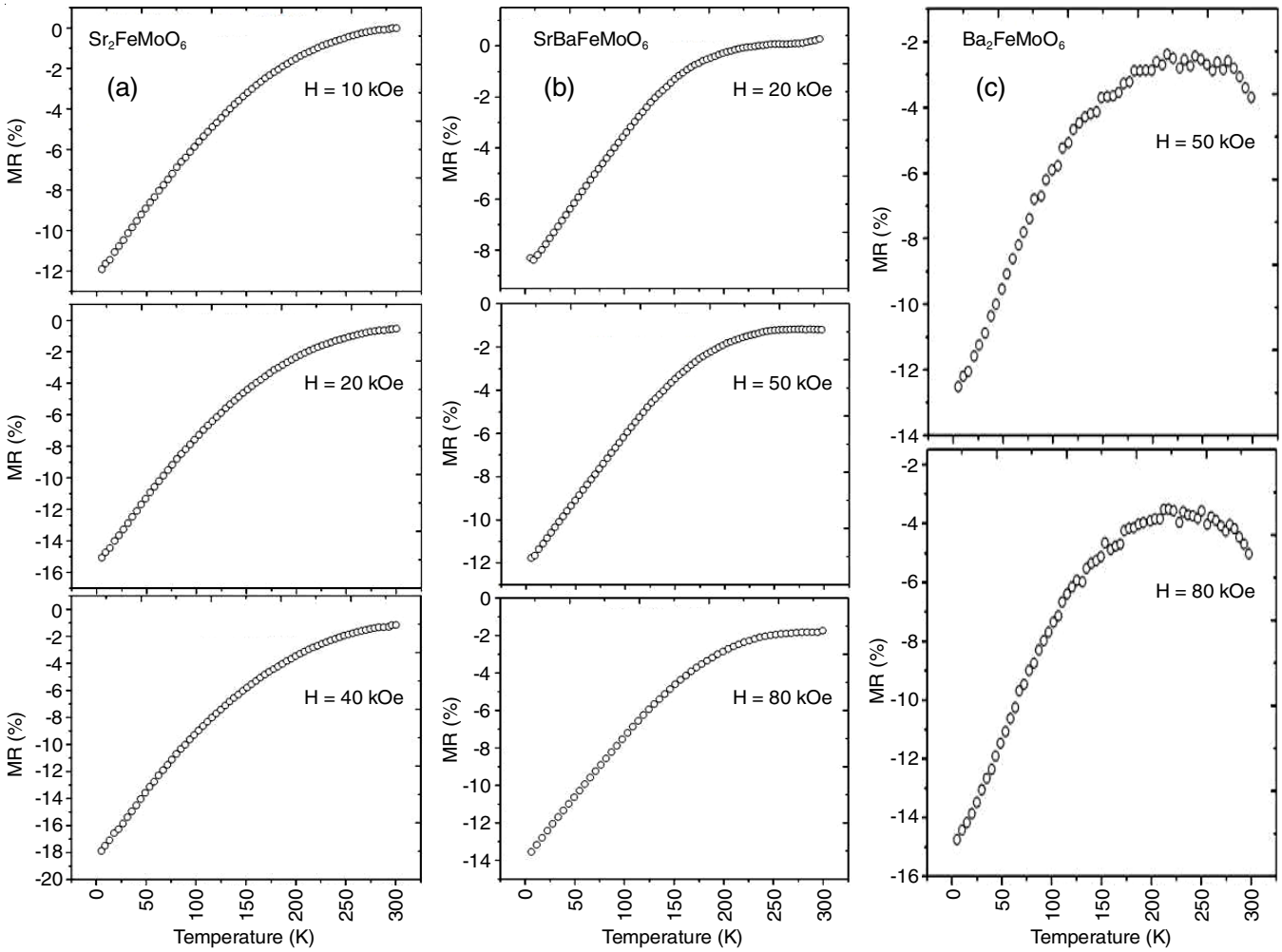

Fig. 5. Variation of MR (%) with temperature at different magnetic field for composition (a) x = 0, (b) x =1 and (c) x =2 of $Sr_{2-x}Ba_xFeMoO_6$

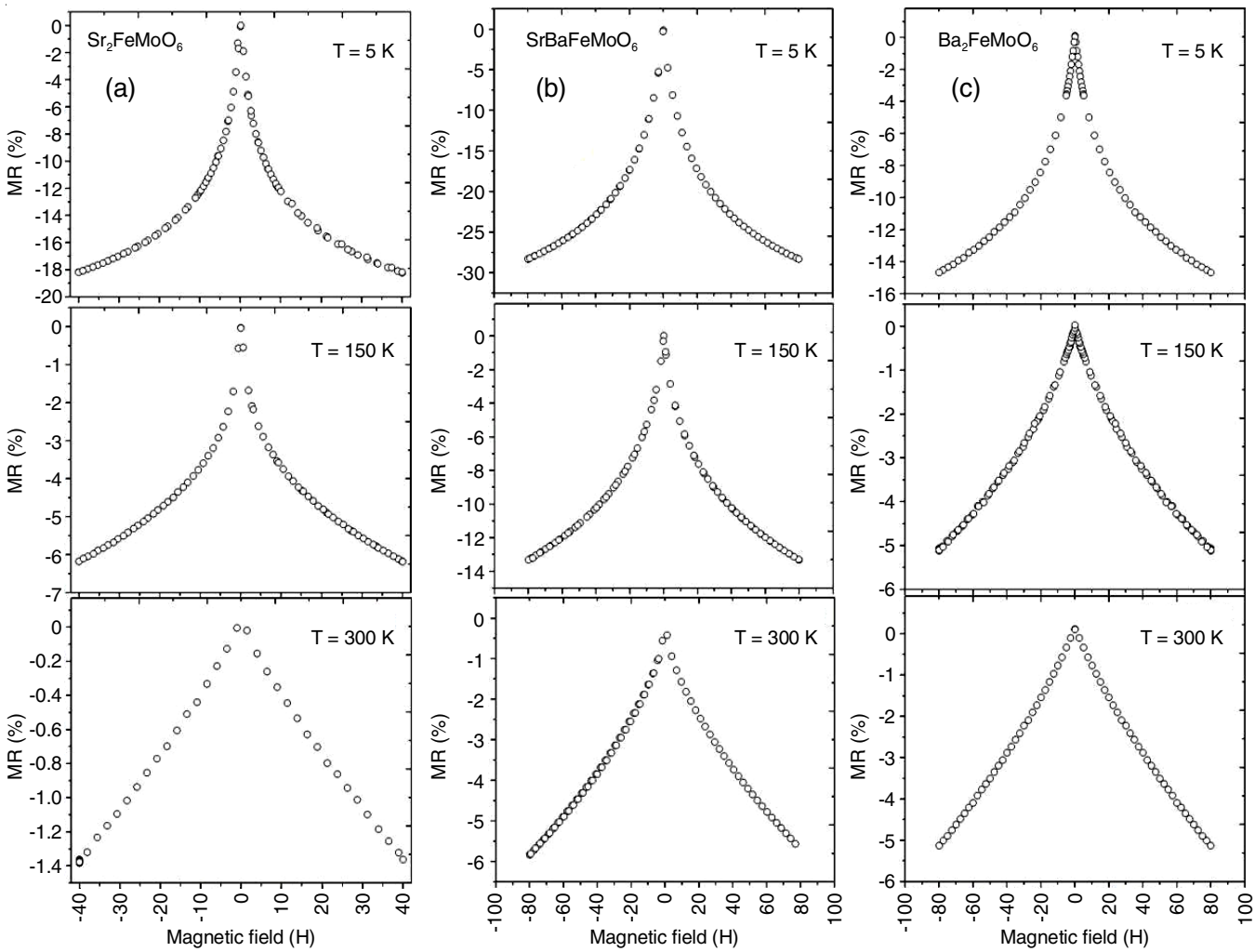

Fig. 6 Variation of MR (%) with magnetic field at temperatures 5, 150 and 300 K for the composition (a) $x = 0$, (b) $x = 1$ and (c) $x = 2$ of $Sr_{2-x}Ba_xFeMoO_6$

role in tunnelling magnetoresistance. High the magnetic smoothness of the substance, it has the more significant role to increase the low field magneto resistance [4]. In double perovskites, the spin polarization is very sensitive to anti-site defects as well as temperature.

Composition dependence magnetoresistance and magnetization: The values of MR (%) with composition at temperature and magnetic field (5 K and 20 kOe), (150 K and 40 kOe) and (300K and 40 kOe) are shown in Fig. 7a. The plot of saturation magnetization *versus* composition is illustrated in Fig. 7b. It is understood that the highest value of MR (%) and magnetization occur at $x = 1$ and after which the value of MR (%) and saturation magnetization lowers as composition deviates from $x = 1$. The fall in MR (%) and saturation magnetization while deviating from composition $x = 1$ in $Sr_{2-x}Ba_xFeMO_6$ may be ascribed to attenuation of Fe/Mo-site ordering or anti-site defects growth [5,9, 19,24]. It is observed that the magnitude of MR (%) and M_s are maximum at $x = 1.0$ and also both of them decrease when composition deviates from $x = 1$. Hence, it can be concluded that there is a correlation between, magnetoresistance and magnetic properties with degree of ordering in $Sr_{2-x}Ba_xFeMO_6$.

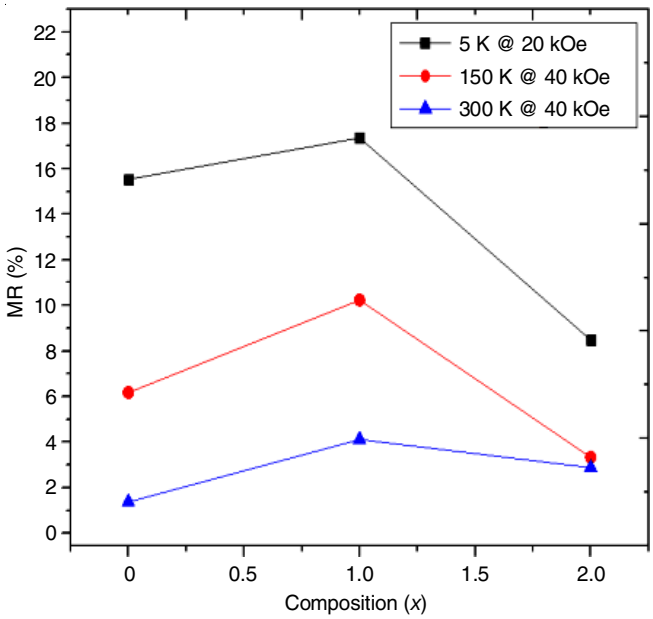

Fig. 7a. The values of magnetoresistance (MR, %) with composition at temperature and magnetic field (5 K and 20 kOe), (150 K and 40 kOe) and (300 K and 40 kOe)

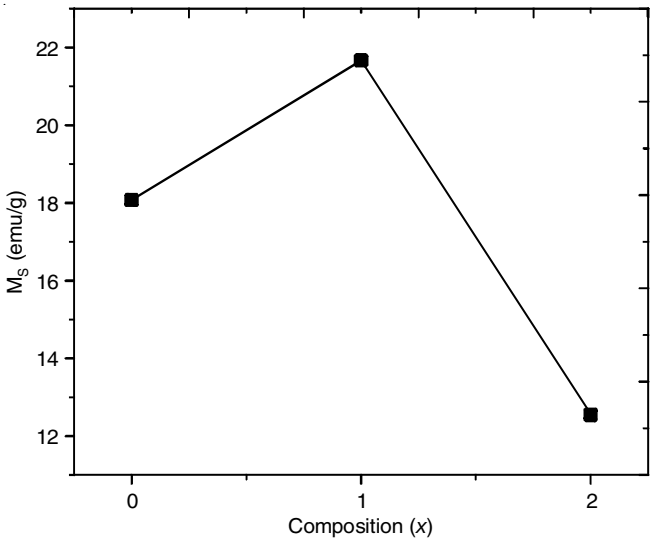

Fig. 7b. Plot of saturation magnetization (M_s) *versus* composition

Conclusion

In this work, the sol-gel process was used to prepare double perovskite $Sr_{2-x}Ba_xFeMoO_6$ (x = 0, 1 and 2) (SBFMO), which was sintered at 1050 ºC in the presence of gas flow (H_2-Ar) for 12 h to convert the ionic state from Mo^{6+} to Mo^{5+}. The lattice parameters and unit cell volume increases with change of composition owing to the size of Ba^{2+} which is bigger than that of Sr^{2+} and it was found that the structural phase transition from tetragonal to cubic lattice occurs at composition x = 1 in SBFMO. The saturation magnetization (M_s) is found to be highest for composition x = 1 and lowers when composition x deviates from 1, which arises by the rise in anti-site defects or decrease in degree of ordering. The samples also show a change from the semiconductor to metallic as temperature varies from 5 to 300 K. The change in value of MR (%) of SBFMO samples increases with lowering the temperature due to effect of the grain boundaries domination or effect of magnetic domain boundaries and increase with an increase in a magnetic field due to the lower of spin collisions at grain boundaries. The magnitude of MR (%) of SBFMO is higher at x = 1 and, then decreases when composition depart from x = 1. From these results, it is confirmed that there is a correlation between the magnetoresistance and magnetic properties with degree of ordering in $Sr_{2-x}Ba_xFeMO_6$.

ACKNOWLEDGEMENTS

The authors thank Dr. Rajeev Rawat, Dr. V. Ganesan Centre, Director of UGC-DAE, Consortium for Scientific Research, Indore, India for providing the magnetoresistance and magnetization facilities. One of the authors, A. Manjula Devi also thanks The Principal and Management of A.V. College of Arts, Science and Commerce, Hyderabad for their encouragement and providing the other necessary facilities.

CONFLICT OF INTEREST

The authors declare that there is no conflict of interests regarding the publication of this article.

REFERENCES

1. K.I. Kobayashi, T. Kimura, H. Sawada, K. Terakura and Y. Tokura, *Nature*, **395**, 677 (1998); https://doi.org/10.1038/27167
2. G.Y. Liu, G.H. Rao, X.M. Feng, H.F. Yang, Z.W. Ouyang, W.F. Liu and J.K. Liang, *Physica B*, **334**, 229 (2003); https://doi.org/10.1016/S0921-4526(03)00070-X
3. B. Jurca, J. Berthon, N. Dragoe and P. Berthet, *J. Alloys Compd.*, **474**, 416 (2009); https://doi.org/10.1016/j.jallcom.2008.06.100
4. V. Pandey, V. Verma, R.P. Aloysius, G.L. Bhalla, V.P.S. Awana, H. Kishan and R.K. Kotnala, *J. Magn. Magn. Mater.*, **321**, 2239 (2009); https://doi.org/10.1016/j.jmmm.2009.01.032
5. Y. Markandeya, D. Saritha, M. Vithal, A.K. Singh and G. Bhikshamaiah, *J. Alloys Compd.*, **509**, 5195 (2011); https://doi.org/10.1016/j.jallcom.2011.02.034
6. A. Gaur, G.D. Varma and H.K. Singh, *J. Alloys Compd.*, **460**, 581 (2008); https://doi.org/10.1016/j.jallcom.2007.06.024
7. T. Goko, Y. Endo, E. Morimoto, J. Arai and T. Matsumoto, *Physica B*, **329-333**, 837 (2003); https://doi.org/10.1016/S0921-4526(02)02537-1
8. H. Han, C.S. Kim and B.W. Lee, *J. Magn. Magn. Mater.*, **254-255**, 574 (2003); https://doi.org/10.1016/S0304-8853(02)00901-0
9. F. Sher, A. Venimadhav, M.G. Blamire, B. Dabrowski, S. Kolesnik and J.P. Attfield, *J. Solid State Sci.*, **7**, 912 (2005); https://doi.org/10.1016/j.solidstatesciences.2005.03.002
10. Y. Markandeya, K. Suresh and G. Bhikshamaiah, *J. Alloys Compd.*, **509**, 9598 (2011); https://doi.org/10.1016/j.jallcom.2011.06.108
11. G. Rajender, Y. Markandeya, K. Suresh, A.K. Singh and G. Bhikshamaiah, *J. Mater. Sci. Mater. Electron.*, **31**, 2877 (2020); https://doi.org/10.1007/s10854-019-02832-6
12. G.Y. Liu, G.H. Rao, X.M. Feng, H.F. Yang, Z.W. Ouyang, W.F. Liu and J.K. Liang, *J. Alloys Compd.*, **353**, 42 (2003); https://doi.org/10.1016/S0925-8388(02)01316-6
13. G.Y. Liu, G.H. Rao, X.M. Feng, H.F. Yang, Z.W. Ouyang, W.F. Liu and J.K. Liang, *J. Phys. Condens. Matter*, **15**, 2053 (2003); https://doi.org/10.1088/0953-8984/15/12/322
14. A.S. Ogale, S.B. Ogale, R. Ramesh and T. Venkatesan, *Appl. Phys. Lett.*, **75**, 537 (1999); https://doi.org/10.1063/1.124440
15. L. Balcells, J. Navarro, M. Bibes, A. Roig, B. Martinez and J. Fontcuberta, *Appl. Phys. Lett.*, **78**, 781 (2001); https://doi.org/10.1063/1.1346624
16. A. Peña, J. Gutierrez, L.M. Rodríguez-Martínez, J.M. Barandiarán, T. Hernández and T. Rojo, *J. Magn. Magn. Mater.*, **254-255**, 586 (2003); https://doi.org/10.1016/S0304-8853(02)00905-8
17. D. Niebieskikwiat, A. Caneiro, R.D. Sánchez and J. Fontcuberta, *Physica B*, **320**, 107 (2002); https://doi.org/10.1016/S0921-4526(02)00655-5
18. D. Kumar and D. Kaur, *Physica B*, **405**, 3259 (2010); https://doi.org/10.1016/j.physb.2010.04.056
19. M. Garcia-Hernandez, J.L. Martinez, M.J. Martinez-Lope, M.T. Casais and J.A. Alonso, *Phys. Rev. Lett.*, **86**, 2443 (2001); https://doi.org/10.1103/PhysRevLett.86.2443
20. D.M. Evans, M. Alexe, A. Schilling, A. Kumar, D. Sanchez, N. Ortega, R.S. Katiyar, J.F. Scott and J.M. Gregg, *Adv. Mater.*, **27**, 6068 (2015); https://doi.org/10.1002/adma.201501749
21. A. Kumar, G.L. Sharma, R.S. Katiyar, R. Pirc, R. Blinc and J.F. Scott, *J. Phys. Condens. Matter*, **21**, 382204 (2009); https://doi.org/10.1088/0953-8984/21/38/382204
22. M. Itoh, I. Ohta and Y. Inaguma, *Mater. Sci. Eng. B*, **41**, 55 (1996); https://doi.org/10.1016/S0921-5107(96)01623-6
23. Y.M. Yutaka Moritomo, H.K. Hiroyuki Kusuya, T.A. Takumi Akimoto and A.M. Akihiko Machida, *Jpn. J. Appl. Phys.*, **39**, L360 (2000); https://doi.org/10.1143/JJAP.39.L360
24. X.M. Feng, G.H. Rao, G.Y. Liu, W.F. Liu, Z.W. Ouyang and J.K. Liang, *J. Phys. Condens. Matter*, **16**, 1813 (2004); https://doi.org/10.1088/0953-8984/16/10/013